Single-Pixel Imaging with Heralded Single Photons

Steven D Johnson (steven.johnson@glasgow.ac.uk)
University of Glasgow
Alex McMillan
University of Bristol
Cyril Torre
University of Bristol
Stefan Frick
Institute for Quantum Optics and Quantum Information Innsbruck
John Rarity
University of Bristol
Miles J. Padgett
University of Glasgow

Research Article

Keywords: Single-pixel imaging, photons, Traditional remote sensing, llumination, noise, contrast images

Posted Date: December 20th, 2021

DOI: https://doi.org/10.21203/rs.3.rs-1160001/v1

Version of Record: A version of this preprint was published at Optics Continuum on March 22nd, 2022.
See the published version at https://doi.org/10.1364/OPTCON.458248.

Single-pixel imaging with heralded single photons

Steven D. Johnson[1,*], Alex McMillan[2], Cyril Torre[2,3], Stefan Frick[4], John Rarity[2], and Miles J. Padgett[1]

[*]steven.johnson@glasgow.ac.uk
[1]School of Physics and Astronomy, University of Glasgow, Glasgow, G12 8QQ, United Kingdom
[2]Quantum Engineering Technology Labs, H. H. Wills Physics Laboratory and Department of Electrical and Electronic Engineering, University of Bristol, BS8 1FD, United Kingdom
[3]Quantum Engineering Centre for Doctoral Training, Nanoscience and Quantum Information Centre, University of Bristol, BS8 1FD, United Kingdom
[4]Institut für Experimentalphysik, Universität Innsbruck, Technikerstraße 25, 6020 Innsbruck, Austria

ABSTRACT

Traditional remote sensing applications are often based on pulsed laser illumination with a narrow linewidth and characteristic repetition rate, which are not conducive to covert operation. Whatever methods are employed for covert sensing, a key requirement is for the probe light to be indistinguishable from background illumination. We present a method to perform single-pixel imaging that suppresses the effect of background light and hence improves the signal-to-noise ratio by using correlated photon-pairs produced via spontaneous parametric down conversion. One of the photons in the pair is used to illuminate the object whilst the other acts as a temporal reference, allowing the signal photons to be distinguished from background noise. This heralding method shows how the noise regime is key to producing higher contrast images.

Introduction

The ability to covertly illuminate a scene is a sought-after goal within remote sensing. For covert imaging, there is a requirement that the probe photons be indistinguishable from the fluctuations of the background light. Using a pulsed laser makes this disguise difficult since the defined wavelength and repetition rates allows the source to be distinguished from the background light. In contrast a source based on spontaneous parametric down conversion (SPDC) creates photons over a range of wavelengths at random times, making it a much better candidate for a covert system[1]. There have been recent developments in producing high-flux photon-pair light sources with a broad gain bandwidth that enable this covert probing of a scene to be performed[2].

Using quantum correlations to improve the signal-to-noise (SNR) of imaging has been the subject of significant study[3–6] and with array sensors it has been possible to demonstrate sub-shot noise measurements using a photon-pair light source[7–9]. These correlated photons have also been utilised to distinguish signal photons from the noise photons in the background light and has been applied in a LIDAR system for range finding[10]. Indeed, a further advantage of this approach is since it is based upon random, albeit correlated, events that two or more similar systems can operate in the same environment and not suffer from cross-talk[2,11].

Here we quantify the improvement in SNR in a single-pixel imaging (SPI) system[12,13] by utilising the correlations from a photon-pair light source. SPI has been demonstrated at a variety of wavelengths[14–16], for high speed applications[17,18], and performing depth measurements[19]. In SPI a series of patterns are projected onto a target, the total power of the corresponding transmitted or back-scattered light is measured using a single-pixel detector revealing the overlap between the projected pattern and the object[20]. This method of using a single-pixel to image an unknown scene was developed alongside the field of ghost imaging, where corrected photons were used to produce images with single element detectors as a heralding system with a detector array used to identify the position of the anti-correlated photons[21], this was also shown to also be possible with classical sources[22].

We demonstrate that there exists a noise regime where there is an improvement in the SNR of the images when using the photon-pair, correlated, light source. This will enable the system to be used more covertly in the presence of background light. We present a model and experimental measurements to demonstrate the operating regime where there can be an advantage via correlation.

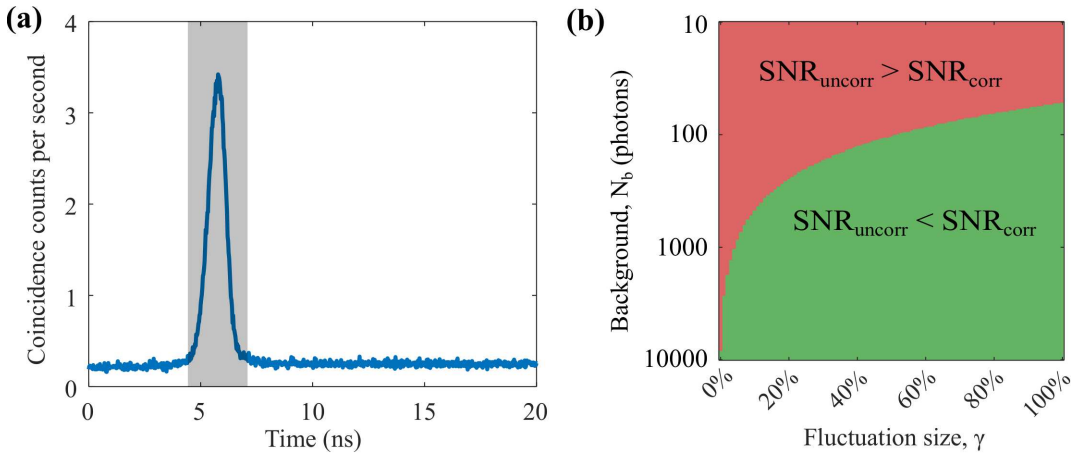

Figure 1. **(a)** Time signal showing the first 20 ns of the temporal correlation measurement with our system with minimal background light present (averaged for 512 seconds). The grey area shows the region determined to be correlated photons. The counts outside of the correlation peak are from accidental photons from the source and background light. **(b)** A plot of the regions where there is higher SNR for the correlated and uncorrelated measurements as calculated from the model, using variables determined from our experimental system.

Measurement principle

In a classical SPI system a light source is used with an optical modulator to produce a structured illumination[23] or is used with a detector to produce a structured detection[24]. In the system presented here SPDC is used to realise a photon-pair light source. The photon-pairs are split such that one is directed to the heralding detector and the other to probe an object with a second detector behind the object, in principle this would be applicable to the back-scattered imaging arrangement, but this is technologically more challenging to implement due to the high losses involved. Outputs from the two detectors are used as stop-start triggers for a coincidence counter. A key parameter to achieve an advantage for the heralding measurement is to maximise the number of two-fold correlated photons. In principle the system can be used in two ways: firstly, the correlations can be ignored and the signal can be read as the total photon count from the signal detector, or secondly the correlations can be used such that the signal is read as only the counts recorded in the coincidence peak. In the first case the signal is maximised but is also subject to being confused by any background light, in the second case, the time gating means most of the background light is eliminated but at the expense of a reduced signal. It is the interplay between these two competing issues that determines the regimes in which using the source correlation might bring an advantage.

The noise in the imaging system will be proportional to the noise from a non-imaging measurement, such that we can estimate the noise in our system. The SNR of our measurement for a given integration time is given by $\mathrm{SNR} = \frac{S}{\sqrt{S+N}}$, where S is the number of counts due to signal photons and N is any additional counts arising from background noise. For the measurement where the correlations are not used (uncorrelated photons), the signal S is the total number of counts detected from the source and the noise is made up from detector dark counts N_d, and the number of measured optical background counts N_b. For any real-world measurements outside of a laboratory the background levels will fluctuate due to varying frequencies of electronics and movement in position of illumination sources, this is included as temporal changes in the background level. To emulate these temporal fluctuations a fluctuation term γ is added, where γN_b is the standard deviation in the background level with a mean value of N_b. The addition of this fluctuation will result in a larger variance than measured from a Poissonian noise source. Therefore, the SNR of our uncorrelated measurement is given by

$$\mathrm{SNR}_{\mathrm{uncorr}} = \frac{S}{\sqrt{S+N_b+N_d}+\gamma N_b}$$

The advantage of using the correlation peak is minimising this background noise due to the gate time associated with the peak, the fraction of the noise falling within the gate time is ε. The coincidence ratio, the fraction of the coincidence counts divided by the total number of counts, is given by h. When using the correlation peak the number of signal counts is reduced to hS. Including the correlation ratio and the time-gating noise reduction enables the correlated SNR to be estimated as

$$\mathrm{SNR}_{\mathrm{corr}} = \frac{hS}{\sqrt{(hS+\varepsilon(N_b+N_d)}+\varepsilon\gamma N_b}$$

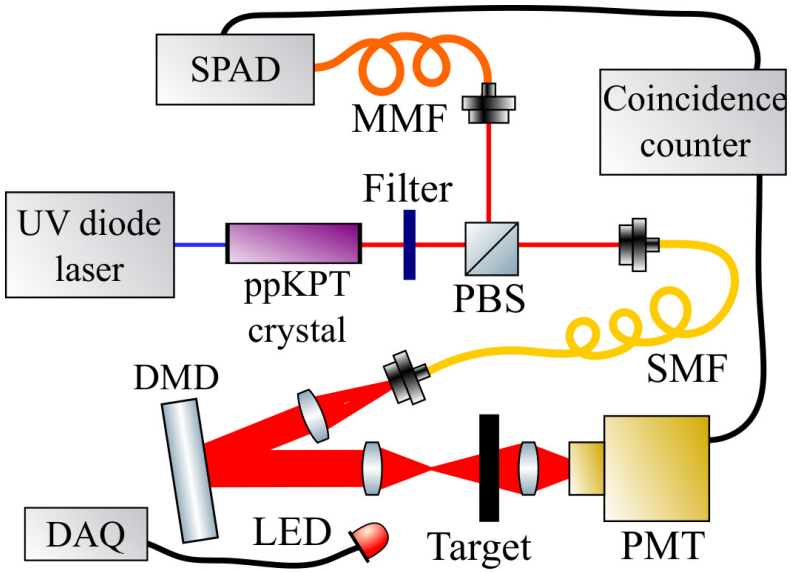

Figure 2. The SPI experimental set up. The SPDC crystal produces 2-photons, one of which is measured by a SPAD detector as a heralding arm, the other is reflected from the DMD acting as a transparency mask, the photons transmitted through the target are recorded with a PMT. The coincidence measurement is made with a coincidence counter.

An example of the temporal measurement of the correlated photons is shown in figure 1(a), with h calculated as the counts contained in the grey period divided by the total number of counts. Figure 1(b) shows the SNR calculated for a range of background and fluctuation levels for both the correlated and uncorrelated cases. For the model the values of $S = 1000$ counts, $N_d = 100$ counts, $h = 0.15$ and $\varepsilon = 0.006$ were used. When there is a higher fluctuating background light level the correlation measurement will have a higher SNR than the uncorrelated case. As figure 1(b) shows, the correlated measurement does not outperform the uncorrelated measurement for all possible parameters. The advantage for the correlated measurement is most apparent when the coincidence ratio h is sufficiently large relative to the inverse gate width ε. For the experimental parameters we report in this paper, we find there is no measurable advantage when using a static background signal ($\gamma = 0$) for noise levels lower than 8 times the signal level.

Experimental methodology

A schematic of the experimental system is shown in figure 2 Our system comprises of a SPDC source of time-correlated photons-pairs, full details can be found in our previous work[2]. Light from a 405 nm laser diode is focused with an aspheric lens into a 30 mm long periodically poled potassium titanyl phosphate (ppKTP) non-linear crystal. The size of the crystal poling structures are linearly chirped between 9.0 µm and 13.0 µm, such that a continuous spectrum is produced to mimic the spectrum of background light, with both signal and idler photons spanning the range 700 nm to 950 nm. Anti-correlation in the wavelength of the pair-photons due to the energy conservation could be used with separate wavelength bandwidth channels to improve measurement sensitivity, however this was not performed in this experiment. The pump light is removed with a long-pass filter, the orthogonal polarized signal and heralding photons are subsequently separated on a polarizing beam-splitter (PBS). These photons are focused into optical fibres to allow distribution from the system. For heralding photons, the light is focused into a multi-mode fiber (MMF) that is connected to a fiber-coupled single-photon avalanche detector (SPAD) detector (Excelitas Photon Counting Module SPDM CD 3416 H). For the signal photon a single-mode fiber (SMF) is used such that, after collimation with a lens, a well-defined near Gaussian beam is obtained for illuminating the object. A digital micro-mirror device (DMD), Vialux V-7001, acts as a transmission mask to pattern the light projected on to the object. The transmission object used was a three-sided star cut into cardboard. For collection of the signal photons a Horiba PPD900 photomultiplier tube (PMT) is used. The photon counting is performed with a Picoquant TimeHarp260, acting as a coincidence counter. To ensure the background light level can be controlled the DMD, target, and detector are installed within a light-tight enclosure. The background light is adjusted using a red LED ($\lambda = 650$ nm), which is connected to a National Instruments USB-6211 DAQ. The voltage on the LED is used to set the intensity level, which was calibrated from measurements from the number of photons measured by the PMT for a given voltage. As the signal measurement is not spatially resolved the measured data is largely unaffected by the exact positioning of the LED within the enclosure.

Careful alignment of the SPDC system is required to ensure a high correlation ratio, a value of 15% was achieved with

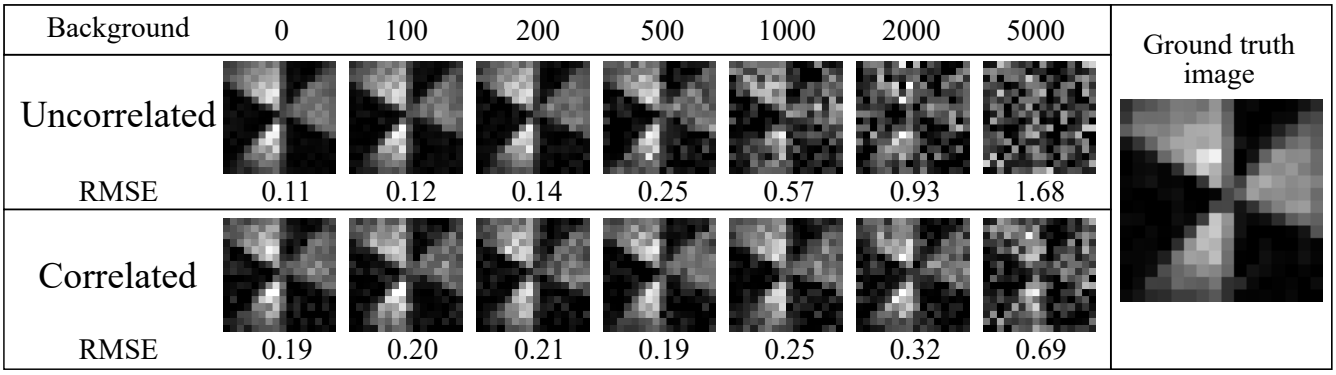

Figure 3. An example of the images produced for both the correlated and uncorrelated measurements with the SPDC system. The data shown are for the fluctuation magnitude $\gamma = 30\%$ and varying background photon level. The root mean squared error (RMSE) calculated for each measurement is shown below each image.

the experimental system presented. For our source, the heralding photons were measured via a MMF (50 µm core diameter), the average photon level measured is 8×10^6 cps (counts per second). For target illumination a SMF is used (5.6 µm core diameter), which transmits 6 times fewer photons. The PMT for detection has a much lower quantum efficiency than the SPAD (1% compared to 65% for our wavelength range), there is loss due to the DMD (20% reflected) and the target is approximately 50% transparent. Therefore, the average signal after the losses is 1000 cps. Optimal collection of photons for maximising the correlation ratio will occur when SMF are used in both the signal and heralding arm. However, there is an increase in heralding photons if a larger optical fibre is used, but this reduces the correlation ratio.

The pattern set implemented on the DMD is the Hadamard basis[13,25], where for each pattern a measurement is made for both the positive and photographic negative patterns, the difference between these two values being the signal used in the image reconstruction. For the uncorrelated case the signal is the total number of counts and for the correlated case the signal is the the number of counts in the coincidence peak. The SPI images is calculated as the differential signal for each pattern multiplied by the Hadamard matrix, the subsequent vector of the pixel values is reshaped to a square image. The Hadamard pattern size and number of illumination trials were chosen to generate a final combined output image of 16×16 pixels. With SPI compressive sensing can be used to reduce the number of measurements required[12], this would make a comparison of noise more difficult so a full sampling basis was performed for these measurements.

To produce fluctuations in the background the LED voltage was adjusted for each individual pattern measurement. The LED voltage is set to give a signal with a mean equal to the background level N_b and a standard deviation of the fluctuation level γ multiplied by N_b and a random value determined by a normal noise distribution, this value is truncated to zero for negative numbers of photons. The background light from the LED is set at the start of each measurement of a new pattern to simulate a varying photon background level. Changing at a faster rate than this would nullify the effect of the changes due to averaging, therefore this is a 'worst case'. For the measurement each pattern was recorded over a 1 second acquisition for 512 patterns for a 16×16 image (8½ minutes per acquisition). The measurement was repeated for each background level and each fluctuation level between 0% and 100%. As the fluctuation level is a percentage of the background, for a zero background level there was no background fluctuation.

To enable a comparison of the results obtained from uncorrelated or correlated measurements a ground truth image was acquired. The existing SPI system was used with a significantly higher illumination light level, a Helium-Neon laser was input into the single-mode fibre and was adjusted to give approximately 10^6 cps at the signal detector. This ground truth image of our target therefore naturally incorporates the Gaussian shape of the illumination beam that contributes to the varying intensity within the image and any image degradation due to finite resolving power of the optical system, allowing for a direct comparison of the correlated and uncorrelated strategies under the same realistic conditions of image degradation.

Results

SPI measurements were performed for a range of values of the background and fluctuation levels. Without background illumination an average signal level of 1000 cps was recorded for each measurement. The background photon level was increased from 0 up to a level of 20 000 photons, the fluctuation size was adjusted between 0% and 100%.

The root mean squared error (RMSE) of the image reconstruction is calculated with respect to the ground truth image. The RMSE is calculated by first normalising the ground truth and reconstructed images by subtracting the mean value from each individual pixel and dividing by the standard deviation. The reconstructed N-pixel image x is compared to the ground

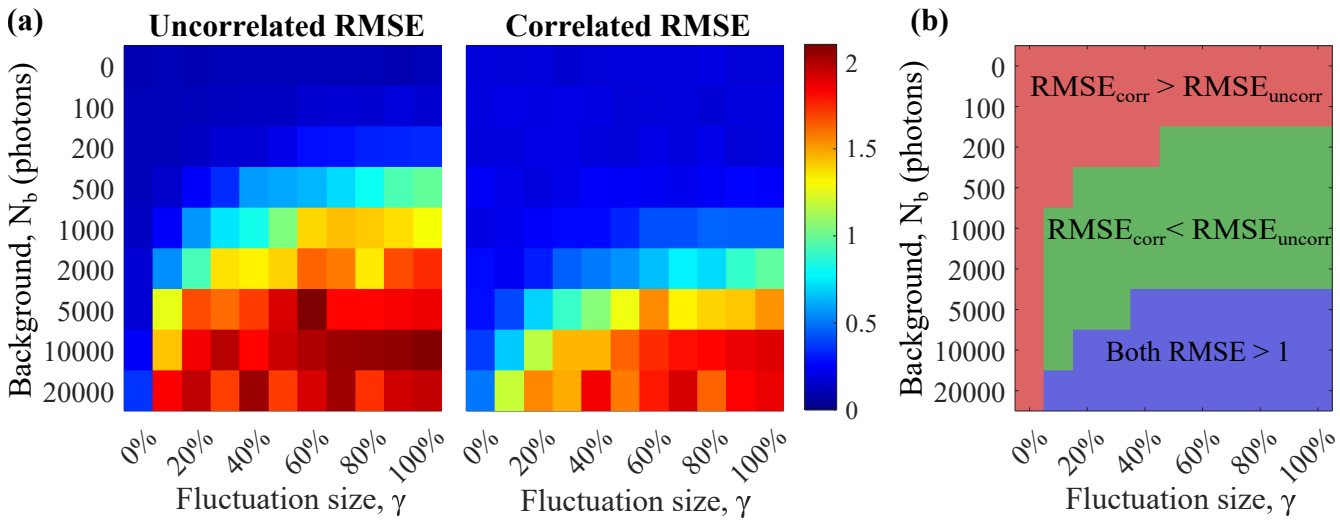

Figure 4. **(a)** The RMSE calculated for the reconstructed image for the full range of measurements for varying the average photon background level and the size of fluctuation in the background during the acquisition of both the uncorrelated and correlated image. **(b)** A comparison of the correlated and uncorrelated images to determine under what parameters there is an advantage to using the heralding.

truth image x_{gt} calculated as RMSE $= \sqrt{\sum_{n=1}^{N}(x_n - x_{gt,n})^2/N}$. Example images from the data set are presented in figure 3, the images are shown for a fluctuation magnitude $\gamma = 30\%$, where the background level is varied. Figure 4 presents the RMSE values for all measurements. The values of correlated (RMSE$_{corr}$) and uncorrelated (RMSE$_{uncorr}$) error measurements are compared and highlighted in figure 4(b). It is shown that for higher background levels there is higher RMSE in the uncorrelated measurement. It was decided that images were too noisy to identify when both RMSE > 1 (an average error greater than 1 for each pixel in the normalised image) and neither measurement method is a valid way to acquire the image under this condition. It can be seen there are a wide range of values where the correlated measurement has an advantage over the uncorrelated measurement. There is significant agreement between our model presented in figure 1(b) and the measurements in figure 4.

Discussion

The application of this system would be to enable sensing in a covert manner. For use outside of the laboratory there would need to be consideration of the ambient light levels and the fluctuations under these conditions. The key improvement of the temporally correlated sensing is for removal of a fluctuating background signal, the straight-forward solution to this would be to adjust the measurement time to be longer than the temporal fluctuation time of the background, there by minimising any improvement from the correlations. If the methodology were implemented significant improvement in the hardware would be required, if we assume a heralding rate $h = 1$ and assuming relatively small detector noise we would still require a very high photon flux from our source. For example, the source would need comparable output to background light, where source levels as low as 100 times lower than background could be used. As incident light levels vary with conditions an exact number of background photons is difficult to determine, however for an overcast night sky we can assumed irradiance of 10^7 photons per second per square millimetre could be considered. Therefore, for a detection with a 1 mm^2 detector a photon flux of 10^5 would be needed at detection, where losses in the projection, scattering and measurement (based on our system of 10^3 loss) would require an initial flux of 10^8, around 2 orders of magnitude greater than our current system. Another limitation will be detector saturation and electronic data transfer, both are limited to the range of 10^7 to 10^8, these would be saturated by background light with current sources without optical filtering. Suitable optical bandpass filters could be used to reduce the ambient light, but the broadband source gives the greatest advantage for covert operations, therefore there is a trade-off between removing background light and covertness. To perform this measurement in the back scattered direction we would need to consider the Lambertian scattering, with reduction in light reducing as a function of the distance to the object squared, this would produce losses of 60-100 dB for measurement in the range of metres to 1 km[26]. Whilst there may be advantage in the correlation method there are significant real-world problems that significantly reduce its effectiveness.

Conclusion

The model and experimental data have both shown the benefit to using a photon-pair heralding system for single pixel imaging in the presence of background light. Introducing fluctuating background noise leads to a regime where the correlations in a photon pair source can improve the RMSE. Irrespective of using uncorrelated or correlated measurements there is a noise level where the RMSE increases to the point where it is no longer able to recover an image of the object. The limitation on the correlation measurement is down to the heralding efficiency and the maximum detectable photon rate, limited by either the photon source or detector saturation rate. However, in general heralding can give an advantage when heralding rates are not high compared to the inverse gate time. There are technological limitations due to the maximum count rate of detectors, reducing the heralding rate would increase the heralding efficiency. For remote sensing there is the significant reduction in the number of measured photons due to the huge geometrical losses associated with the collection of back-scattered light and therefore a source with a greater number of photon-pairs would be required.

References

1. Rarity, J. G., Tapster, P. R., Walker, J. G. & Seward, S. Experimental demonstration of single photon rangefinding using parametric downconversion. *Appl. Opt.* **29**, 2939–2943, DOI: 10.1364/AO.29.002939 (1990).
2. Frick, S., McMillan, A. & Rarity, J. Quantum rangefinding. *Opt. Express* **28**, 37118–37128, DOI: 10.1364/OE.399902 (2020).
3. Lloyd, S. Enhanced sensitivity of photodetection via quantum illumination. *Science* **321**, 1463–1465, DOI: 10.1126/science.1160627 (2008). https://science.sciencemag.org/content/321/5895/1463.full.pdf.
4. Lopaeva, E. D. *et al.* Experimental realization of quantum illumination. *Phys. Rev. Lett.* **110**, 153603, DOI: 10.1103/PhysRevLett.110.153603 (2013).
5. Moreau, P.-A. *et al.* Demonstrating an absolute quantum advantage in direct absorption measurement. *Sci. Reports* **7**, 6256, DOI: 10.1038/s41598-017-06545-w (2017).
6. Gregory, T., Moreau, P.-A., Toninelli, E. & Padgett, M. J. Imaging through noise with quantum illumination. *Sci. Adv.* **6**, DOI: 10.1126/sciadv.aay2652 (2020). https://advances.sciencemag.org/content/6/6/eaay2652.full.pdf.
7. Sabines-Chesterking, J. *et al.* Sub-shot-noise transmission measurement enabled by active feed-forward of heralded single photons. *Phys. Rev. Appl.* **8**, 014016, DOI: 10.1103/PhysRevApplied.8.014016 (2017).
8. Sabines-Chesterking, J. *et al.* Twin-beam sub-shot-noise raster-scanning microscope. *Opt. Express* **27**, 30810–30818, DOI: 10.1364/OE.27.030810 (2019).
9. Brida, G., Genovese, M. & Ruo Berchera, I. Experimental realization of sub-shot-noise quantum imaging. *Nat. Photonics* **4**, 227–230, DOI: 10.1038/nphoton.2010.29 (2010).
10. Ren, X. *et al.* Time-of-flight depth-resolved imaging with heralded photon source illumination. In *Conference on Lasers and Electro-Optics*, AM3K.6, DOI: 10.1364/CLEO_AT.2020.AM3K.6 (Optical Society of America, 2020).
11. Amann, M.-C., Bosch, T. M., Lescure, M., Myllylae, R. A. & Rioux, M. Laser ranging: a critical review of unusual techniques for distance measurement. *Opt. Eng.* **40**, 10–19, DOI: 10.1117/1.1330700 (2001).
12. Duarte, M. F. *et al.* Single-pixel imaging via compressive sampling. *IEEE Signal Process. Mag.* **25**, 83–91, DOI: 10.1109/MSP.2007.914730 (2008).
13. Gibson, G. M., Johnson, S. D. & Padgett, M. J. Single-pixel imaging 12 years on: a review. *Opt. Express* **28**, 28190–28208, DOI: 10.1364/OE.403195 (2020).
14. Zhang, J., Wang, Q., Dai, J. & Cai, W. Demonstration of a cost-effective single-pixel uv camera for flame chemiluminescence imaging. *Appl. Opt.* **58**, 5248–5256, DOI: 10.1364/AO.58.005248 (2019).
15. Edgar, M. P. *et al.* Simultaneous real-time visible and infrared video with single-pixel detectors. *Sci. Rep.* **5**, 10669, DOI: 10.1038/srep10669 (2015).
16. Stantchev, R. I., Yu, X., Blu, T. & Pickwell-MacPherson, E. Real-time terahertz imaging with a single-pixel detector. *Nat. Commun.* **11**, 2535, DOI: 10.1038/s41467-020-16370-x (2020).
17. Xu, Z.-H., Chen, W., Penuelas, J., Padgett, M. & Sun, M.-J. 1000 fps computational ghost imaging using LED-based structured illumination. *Opt. Express* **26**, 2427–2434, DOI: 10.1364/OE.26.002427 (2018).
18. Johnson, S. D., Phillips, D. B., Ma, Z., Ramachandran, S. & Padgett, M. J. A light-in-flight single-pixel camera for use in the visible and short-wave infrared. *Opt. Express* **27**, 9829–9837, DOI: 10.1364/OE.27.009829 (2019).

19. Sun, M.-J. *et al.* Single-pixel three-dimensional imaging with time-based depth resolution. *Nat. Commun.* **7**, 12010, DOI: 10.1038/ncomms12010 (2016).

20. Sun, B., Welsh, S. S., Edgar, M. P., Shapiro, J. H. & Padgett, M. J. Normalized ghost imaging. *Opt. Express* **20**, 16892–16901, DOI: 10.1364/OE.20.016892 (2012).

21. Bennink, R. S., Bentley, S. J., Boyd, R. W. & Howell, J. C. Quantum and classical coincidence imaging. *Phys. Rev. Lett.* **92**, 033601, DOI: 10.1103/PhysRevLett.92.033601 (2004).

22. Bennink, R. S., Bentley, S. J. & Boyd, R. W. "two-photon" coincidence imaging with a classical source. *Phys. Rev. Lett.* **89**, 113601, DOI: 10.1103/PhysRevLett.89.113601 (2002).

23. Shapiro, J. H. Computational ghost imaging. *Phys. Rev. A* **78**, 061802, DOI: 10.1103/PhysRevA.78.061802 (2008).

24. Yu, W.-K. *et al.* Complementary compressive imaging for the telescopic system. *Sci. Rep.* **4**, 5834, DOI: 10.1038/srep05834 (2014).

25. Zhang, Z., Wang, X., Zheng, G. & Zhong, J. Hadamard single-pixel imaging versus Fourier single-pixel imaging. *Opt. Express* **25**, 19619–19639, DOI: 10.1364/OE.25.019619 (2017).

26. McCarthy, A. *et al.* Kilometer-range, high resolution depth imaging via 1560 nm wavelength single-photon detection. *Opt. Express* **21**, 8904–8915, DOI: 10.1364/OE.21.008904 (2013).

Acknowledgements

The authors would like to acknowledge Jonathan Mathews for useful discussions. The authors gratefully acknowledge financial support from the Engineering and Physical Sciences Research Council (EPSRC) EP/T00097X/1 and EP/S026444/1, and the Quantum Engineering Centre for Doctoral Training EP/L015730/1).

Author contributions statement

M.J.P. and J.R. conceived the experimental concept. S.D.J. designed the imaging experiment, performed the data acquisition and analysis. A.M. and C.T. assisted with the development of the experimental set up. S.F. and J.R. designed the correlated photon system. S.D.J. and M.J.P. wrote the manuscript and all other authors provided editorial input.

Additional information

Competing interests

The authors declare no competing financial interests.

Data availability

Data underlying the results presented in this paper are available at the University of Glasgow data repository, https://dx.doi.org/10.5525/gla.researchdata.1215.